ISSN 0025-6544, Mechanics of Solids, 2020, Vol. 55, No. 8, pp. 1432–1440. © Allerton Press, Inc., 2020.
Russian Text © The Author(s), 2020, published in Prikladnaya Matematika i Mekhanika, 2020, Vol. 84, No. 5, pp. 663–674.

Multimode Model for Fatigue Damage Development

I. S. Nikitin[a,*], N. G. Burago[a,b,], A. B. Zhuravlev[b,***], and A. D. Nikitin[a,****]**

[a] *Institute for Computer Aided Design, Russian Academy of Sciences, Moscow, 123056 Russia*

[b] *Ishlinsky Institute for Problems in Mechanics, Russian Academy of Sciences, Moscow, 119526 Russia*

**e-mail: i_nikitin@list.ru*

***e-mail: buragong@yandex.ru*

****e-mail: zhuravlev.alex2010@yandex.ru*

*****e-mail: nikitin_alex@bk.ru*

Received May 18, 2020; revised July 15, 2020; accepted July 21, 2020

Abstract—A multimode kinetic model for the development of damage under cyclic loading is proposed to describe the development of fatigue failure process. To determine the coefficients of the kinetic damage equation, the well-known Smith–Watson–Topper (SWT) criterion of multiaxial fatigue fracture is used. On this basis, a procedure for calculating the kinetic equation coefficients for various modes of fatigue failure from low-cycle to very-high-cycle fatigue is proposed. A uniform numerical method is developed and examples of calculating the development of crack-like zones of damage and fatigue fracture of samples containing various defects for different cyclic loading modes are presented.

Keywords: fatigue failure, high-cycle fatigue, very-high-cycle fatigue, multimode model, damage equation, fracture criterion

DOI: 10.3103/S002565442008021X

INTRODUCTION

Two main problems of the theory of fatigue failure exist: determining the local zone and the number of loading cycles to the generation of fatigue cracks, as well as determining the rate and direction of their development before their coming to at the surface of a sample or a structural element and final macrofailure.

The main approaches to solve these problems in the case of multiaxial cyclic loading are related with tests of samples, generalization of laws established for uniaxial loadings and described by the fatigue S–N Wohler-type curves and the Basquin-type relations [1].

A large number of criteria (stress-based criteria) are based on the direct generalization of S–N curves constructed from the results of fatigue tests and divided into two large groups. The first group contains the criteria including the amplitudes of invariant characteristics of the stress state in the loading cycle: octahedral stresses, principal stresses, etc. [2, 3], and the second group contains those criteria which consider the values of amplitudes of tangent and/or normal stresses at the so-called critical plane [4–9]. Usually, this plane is determined from the maximum condition of amplitudes of tangent, normal stresses, or their certain combination over elementary areas of all-possible orientations. The surveys on this topic are presented in works [10–13].

Two approaches to study the development processes of fatigue damage zones also exist. The first one is based on classical concepts of the fracture mechanics and associates the development conditions of fatigue cracks at an increasing number of cycles and amplitudes of the stress intensity factors at the tip of the crack. The main equation was proposed by Paris [14] and many modifications exist [15, 16].

The second approach utilizes the ideas of the theory of damage which dates back to works [17, 18] and afterwards developed in [19, 20]. It was applied in [21–23] in application to the problems of cyclic loading and fatigue failure.

In the current work, we propose the multimode model of fatigue damage development based on the evolutionary equation for the damage function. The model parameters are determined for various modes of fatigue damage: low-cycle fatigue (LCF), high-cycle fatigue (HCF), and the very-high-cycle fatigue (VHCF) corresponding to high-frequency low-amplitude loading.

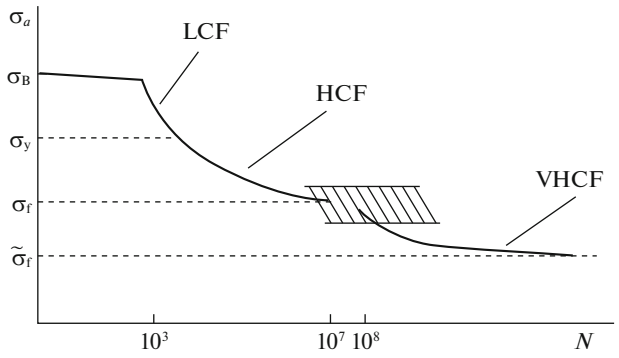

Fig. 1.

To separate different modes of fatigue damage, we use the scheme of multimode amplitude fatigue curve presented in Fig. 1. Until the value $N \sim 10^3$, the mode of repeated static loading is realized with the amplitude close to the static ultimate strength σ_B. Then, the left branch of the bimodal fatigue curve (the Wohler curve) describes the modes of LCF and HCF until $N \sim 10^7$ and the amplitude values near the fatigue strength σ_f. After that, the zone of change begins in the fracture mechanisms and further fall of fatigue strength starting from values $N \sim 10^8$ until the new limiting value $\tilde{\sigma}_f$ according to the right branch of bimodal fatigue S–N curve. This branch describes the VHCF mode [24].

Note that the ideas about explicit separation of the classical Wohler branch into two more parts, LCF and HCF, are being developed today. The boundary of this transition region is determined not by the value N, but by the value of the loading amplitude equal to the yield strength of material σ_y [25], because the physical mechanism of fatigue failure also changes at this transition.

The boundary of repeated static range $N \sim 10^3$ is rather conventional. It is refined in modern studies [25] in dependence on the strength and plastic characteristics of material.

Nevertheless, in the current work we keep the presentation of the proposed model for damage development based on the above discussed scheme.

To make the model consistent with the well-known criteria of multiaxial fatigue failure, we chose the stress-based criterion which describes the fatigue failure related with development of normal opening microcracks. This criterion is the modified Smith–Watson–Topper (SWT) criterion [26, 27], where the dominating role in fatigue damage development is played by amplitudes of maximal tensile stresses. In the original presentation, this and similar stress-based criteria were already applied for describing LCF and HCF modes. An approach was proposed in [24] for generalizing multiaxial failure criteria in describing right branches of fatigue curves in the VHCF mode; this approach uses the reference points of each branch and the inverse power dependence on the number of cycles N to arrive at the asymptote of the fatigue limit. In the current work, we also use this analytical approach to generalize the SWT criterion to the VHCF case.

1. KINETIC EQUATION FOR DAMAGE IN THE LCF–HCF MODE

1.1. The criterion of multiaxial fatigue failure in the LCF–HCF mode with development of microcracks of normal opening (stress-based SWT) corresponding to the left branch of the bimodal fatigue curve (Fig. 1) has the form

$$\sqrt{\langle \sigma_{1_{\max}} \rangle \Delta\sigma_1/2} = \sigma_f + \sigma_L N^{-\beta_{LH}}, \tag{1.1}$$

where σ_1 is the largest principal stress, $\Delta\sigma_1$ is the spread of the largest principal stress in a cycle, and $\Delta\sigma_1/2$ is its amplitude. From the condition of repeated static failure until the values $N \sim 10^3$ using technique [13], we may obtain that $\sigma_L = 10^{3\beta_{LH}}(\sigma_B - \sigma_f)$. According to the chosen failure criterion, only the tensile stresses are involved; therefore, this criterion includes the value $\langle \sigma_{1_{\max}} \rangle = \sigma_{1_{\max}} H(\sigma_{1_{\max}})$, where σ_B is the static ultimate tensile strength of material, σ_f is the classical fatigue strength of material at reverse cycle (the coefficient of cycle asymmetry is $R = \sigma_{\min}/\sigma_{\max} = -1$), β_{LH} is the exponent of the left branch of the bimodal fatigue curve, and $H(x)$ is the Heaviside function.

From the condition of fatigue failure, we obtain the number of cycles to failure at homogeneous stress state,

$$N_{LH} = 10^3 \left[(\sigma_B - \sigma_f)/\left\langle \sigma_{LH} - \sigma_f \right\rangle\right]^{1/\beta_{LH}}, \quad \sigma_{LH} = \sqrt{\left\langle \sigma_{1_{max}} \right\rangle \Delta\sigma_1/2}. \tag{1.2}$$

1.2. To describe development of fatigue damage in the LCF–HCF mode, we introduce the damage function $0 \le \psi(N) \le 1$, which describes the process of gradual cyclic (fatigue) destruction of material. At $\psi = 1$, a material particle is regarded as completely destructed. Its Lamé moduli become equal zero. The damage function ψ in dependence on the number of loading cycles N for the LCF–HCF mode is described by the kinetic equation

$$d\psi/dN = B_{LH}\psi^{\gamma}/(1 - \psi^{\alpha}),$$

where α and $0 < \gamma < 1$ are the model parameters determining the rate of development of fatigue damage. The choice of the denominator in this two-parametric equation prescribes the infinitely large growth rate of the zone of complete destruction at $\psi \to 1$ and is caused by the known experimental data on the kinetic growth curves of fatigue cracks, which have the vertical asymptote and reflect the fact of their explosive, uncontrolled growth at the last stage of macrofailure.

The similar equation for the damage was considered earlier [21, 22]; its multiple parameters and coefficients were determined indirectly by the results of uniaxial fatigue tests. We determine the coefficient B_{LH} by the procedure explicitly associated with the following chosen criterion of multiaxial fatigue failure. By integrating the equation for the damage at uniaxial stress state

$$\left[\psi^{1-\gamma}/(1-\gamma) - \psi^{(1+\alpha-\gamma)}/(1+\alpha-\gamma)\right]\Big|_0^1 = B_{LH}\, N\Big|_0^{N_{LH}},$$

we determine the number of cycles to complete failure N_{LH} at $\psi = 1$

$$N_{LH} = \alpha/(1+\alpha-\gamma)/(1-\gamma)/B_{LH}. \tag{1.3}$$

We equate the values N_{LH} from the failure criterion (1.2) and from the solution to damage Eq. (1.3) and obtain the expression for the coefficient B_{LH}

$$B_{LH} = 10^{-3}\left[\left\langle \sigma_{LH} - \sigma_f \right\rangle/(\sigma_B - \sigma_f)\right]^{1/\beta_{LH}} \alpha/(1+\alpha-\gamma)/(1-\gamma),$$

where the value σ_{LH} is determined by the chosen mechanism of fatigue failure and by the corresponding multiaxial criterion (1.1).

2. KINETIC DAMAGE EQUATION FOR THE VHCF MODE

2.1. The criterion of multiaxial fatigue failure in the VHCF mode corresponding to the right branch of the bimodal fatigue curve in Fig. 2 (the generalized stress-based SWT) has the form

$$\sqrt{\left\langle \sigma_{1_{max}} \right\rangle \Delta\sigma_1/2} = \tilde{\sigma}_f + \sigma_V N^{-\beta_{VH}}, \tag{2.1}$$

where, using the similarity condition of reference points for the left and right branches of the bimodal fatigue curve [24], we may obtain the formula $\sigma_V = 10^{8\beta_{VH}}(\sigma_f - \tilde{\sigma}_f)$.

From the criterion of fatigue failure, we obtain the number of cycles to failure at uniaxial stress state

$$N_{VH} = 10^8 \left[(\sigma_f - \tilde{\sigma}_f)/\left\langle \sigma_{VH} - \tilde{\sigma}_f \right\rangle\right]^{1/\beta_{VH}}, \quad \sigma_{VH} = \sigma_{LH} = \sqrt{\left\langle \sigma_{1_{max}} \right\rangle \Delta\sigma_1/2} \tag{2.2}$$

Here, $\tilde{\sigma}_f$ is the fatigue strength of material at reverse cycle for the VHCF mode and β_{VH} is the exponent of the left branch of the bimodal fatigue curve.

2.2. Similarly to Sect. 1.4 for the VHCF mode, we may determine the coefficient in the damage evolutionary equation

$$d\psi/dN = B_{VH}\psi^{\gamma}/(1 - \psi^{\alpha}), \quad 0 < \gamma < 1.$$

Similarly to Eq. (1.3), we have

$$N_{VH} = \alpha/(1+\alpha-\gamma)/(1-\gamma)/B_{VH}. \tag{2.3}$$

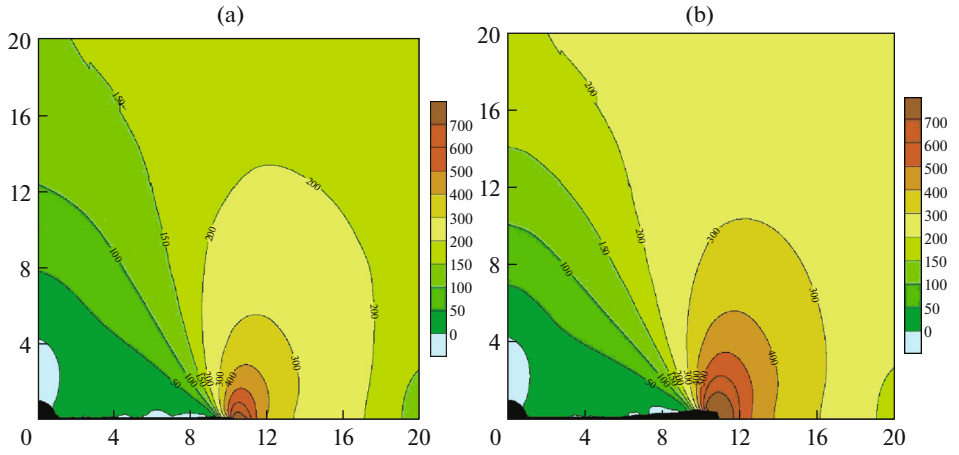

Fig. 2. (a) VHCF mode: $P = 160$ MPa, $N_k = 6.799 \times 10^7$, $N_i = 1.007 \times 10^6$, and $N_f = 6.806 \times 10^7$ and (b) HCF mode: $P = 210$ MPa, $N_k = 3.765 \times 10^6$, $N_i = 7.229 \times 10^4$, and $N_f = 3.807 \times 10^6$.

We equate the values N_{VH} from the failure criterion (2.2) and from the solution to damage Eq. (2.3) and obtain the expression for the coefficient B_{VH} in the damage equation

$$B_{VH} = 10^{-8} \left[\langle \sigma_{VH} - \tilde{\sigma}_f \rangle / (\sigma_f - \tilde{\sigma}_f) \right]^{1/\beta_{VH}} \alpha/(1 + \alpha - \gamma)/(1 - \gamma),$$

where the value σ_{VH} is determined by the chosen mechanism of fatigue failure and by the corresponding multiaxial criterion (2.1).

Behavior of the damaged material is described by the degradation equations of its elasticity moduli $\lambda(\psi) = \lambda_0(1 - \psi)$ and $\mu(\psi) = \mu_0(1 - \psi)$. The material becomes completely destructed and its elasticity moduli vanish when the damage function $\psi(N)$ reaches the value 1.

3. CONDITION FOR SWITCHING MODES OF FATIGUE DAMAGE ACCUMULATION

The transition point from the left branch of the fatigue curve to the right branch at which the mechanism of fatigue failure is changed occurs slightly above the fatigue strength σ_f (Fig. 1) and is determined by the value $\sigma_* = \sigma_f + \Delta\sigma$. To provide continuous matching of the left and right branch of the fatigue curve, we need to fulfill the condition $N_{LH} = N_{VH}$, which is equivalent to the equation for the value $\Delta\sigma$

$$10^3 \left[(\sigma_B - \sigma_f) / \langle \Delta\sigma \rangle \right]^{1/\beta_{LH}} = 10^8 \left[(\sigma_f - \tilde{\sigma}_f) / \langle \sigma_f + \Delta\sigma - \tilde{\sigma}_f \rangle \right]^{1/\beta_{VH}},$$

or

$$\Delta\sigma = 10^{-5\beta_{LH}} (\sigma_B - \sigma_f) \left[1 + \Delta\sigma/(\sigma_f - \tilde{\sigma}_f) \right]^{\beta_{LH}/\beta_{VH}}.$$

Considering the actual smallness of the correction term in the square brackets, we may set the correction value $\Delta\sigma$ by the approximate formula

$$\Delta\sigma = 10^{-5\beta_{LH}} (\sigma_B - \sigma_f).$$

The corresponding approximate value $N_* = N_{LH}(\sigma_*)$ is determined by the value $N_* = 10^3 [(\sigma_{UTS} - \sigma_f)/\Delta\sigma]^{1/\beta_{LH}} \approx 10^8$ as expected.

Using the obtained refined estimates for the transition point between the two branches of the fatigue curve, we obtain the final formulas for the ranges and coefficients of the kinetic damage equations.

For the LCF–HCF mode at $\sigma_f + \Delta\sigma_f < \sigma_{LH} < \sigma_B$ and $\Delta\sigma = 10^{-5\beta_{LH}} (\sigma_B - \sigma_f)$

$$B_{LH} = 10^{-3} \left[\frac{\langle \sigma_{LH} - \sigma_f \rangle}{\langle \sigma_B - \sigma_f \rangle} \right]^{1/\beta_{LH}} \frac{\alpha}{(1 + \alpha - \gamma)(1 - \gamma)}, \quad \sigma_{LH} = \sqrt{\langle \sigma_{1_{max}} \rangle \Delta\sigma_1/2}$$

For the VHCF mode at $\tilde{\sigma}_f < \sigma_{VH} \le \sigma_f + \Delta\sigma_f$

$$B_{VH} = 10^{-8}\left[\frac{\langle\sigma_{VH} - \tilde{\sigma}_f\rangle}{\langle\sigma_B - \tilde{\sigma}_f\rangle}\right]^{1/\beta_{VH}} \frac{\alpha}{(1+\alpha-\gamma)(1-\gamma)}, \quad \sigma_{VH} = \sqrt{\langle\sigma_{1_{max}}\rangle \Delta\sigma_1/2}.$$

At $\sigma_{VH} \le \tilde{\sigma}_f$, there is no fatigue failure whereas at $\sigma_{LH} \ge \sigma_B$, it happens immediately.

4. ALGORITHM FOR COMPUTING FATIGUE DAMAGE

The numerical procedure to solve the differential equation for the damage function consists of the following stages. At the first stage, we compute the stress state of the material's elastic sample in a single loading cycle.

To compute the loading cycle of a deformed sample with defects, we used the Astra software package using the highly economical matrix-less variant of FEM [28] and supplemented by the code for computing the fatigue damage equation and the variation in the elasticity moduli.

Earlier, this FEM variant was applied for developing direct computation methods of the processes of dynamic fracture [29, 30]. In [31], this method was used in constructing the solution algorithms to contact problems. In [32], it was applied for solving the problems of compaction and sintering of samples under quasi-static or nonstationary (non-cycle) loadings.

To integrate the equation $d\psi/dN = B\psi^\gamma/(1-\psi^\alpha)$, $B = B_{LH}, B_{VH}$, we approximated the damage function in the kth node of the computation mesh at the given discrete values of ψ_k^n at the instances N^n and the sought values of ψ_k^{n+1} at the instances N^{n+1}.

Note that, near the state of complete failure at $\psi \to 1$, the denominator of the kinetic equation becomes arbitrarily small and the equation becomes stiff; therefore, the usual explicit methods of its numerical solution are inappropriate. In the numerical solution with the implicit schemes, the nonlinear algebraic system appears in which the solution is demanding in the computation time and achievement of the appropriate accuracy.

Therefore, we chose the following method for computing the damage. We noted that for the value $\alpha = 1 - \gamma$, we may obtain the explicit expression for $\psi_k^{n+1}(\psi_k^n, \Delta N^n)$ using the analytical integration of the kinetic damage equation over the increment of the number of cycles. The kinetic equation becomes one-parametric in this case, but keeps the desirable behavior peculiarities of the damage growth rate (the power growth near zero given by the parameter γ and the infinite growth at $\psi \to 1$).

Let us perform this integration:

$$\frac{\psi^{1-\gamma}}{2(1-\gamma)}[2 - \psi^{1-\gamma}]\Big|_{\psi_k^n}^{\psi_k^{n+1}} = BN\Big|_{N_n}^{N_{n+1}}.$$

We denote $(\psi_k^{n+1})^{1-\gamma} = x$, $q = 2(1-\gamma)B\Delta N^n + (\psi_k^n)^{1-\gamma} - 2(\psi_k^n)^{2(1-\gamma)}$, and $\Delta N^n = N^{n+1} - N^n$ and obtain the equation $x^2 - 2x + q = 0$ and its admissible root $x = 1 - \sqrt{1-q} < 1$. This implies the exact formula for the damage at the increment of the number of cycles ΔN^n:

$$\psi_k^{n+1} = (1 - \sqrt{1 - [2(1-\gamma)B\Delta N^n + (\psi_k^n)^{1-\gamma} - 2(\psi_k^n)^{2(1-\gamma)}]})^{1/(1-\gamma)}.$$

The increment value ΔN^n is determined as follows.

Using the data of stress state computation, we compute the coefficient B for each node. To determine the increment of the number of cycles, we choose the point with the most rapidly increasing damage function, that is, the point where ψ_k^n first increases by a prescribed value $\Delta\psi_0$. The sample is performed over the points where $0 \le \psi_k^n \le 1$. We determine the step value by

$$\Delta N^n = \min_k\left(\frac{\Delta\psi_0(1-\psi_k^n)^{1-\gamma}}{B(\psi_k^n)^\gamma}\right), \quad \psi_k^n > 0,$$

$$\Delta N^n = \min_k\left(\frac{\Delta\psi_0^{1-\gamma}}{B}\right), \quad \psi_k^n = 0.$$

The step value is limited by the given maximum $\Delta N_{\max}$. In the computations, we use the values $\Delta\psi_0 = 0.1$ and $\Delta N_{\max} = 10^5$.

For each node, we consider its current level of damage and equivalent stress and obtain the new level of damage with account for the computed increment ΔN^n.

The degradation of the damaged material was determined in our numerical computations by the relation $E_k^{n+1} = E_0(1 - \psi_k^{n+1})(H(\psi_0 - \psi_k^{n+1}) + 0.001)$, where E_k^{n+1} is the Young modulus at the $(n + 1)$th step in loading cycles at a fixed value of the Poisson coefficient, H is the Heaviside function, and $\psi_0 \sim 1$ is the critical damage parameter at which material transits to the completely destructed state with near-zero elasticity moduli. In the computations, we chose $\psi_0 = 0.9$. The small value of the residual Young modulus for completely destructed material, $0.001E$, plays a role of regularizer and is introduced to keep the possibility of continuous calculation for any damage state.

The computation ends when the region boundaries of completely destructed material emerge at the surface of the sample (macrofailure) or when the evolution of this region terminates.

Using the multimode model and the developed numerical procedure, we solved the problems about development of fatigue damage zones in the neighborhood of typical defects of material structure (microcavities and differently oriented microcracks).

The proposed model and numerical method may be considered the development and generalization of the previously developed algorithms for the direct calculation of the processes of dynamic fracture [29, 30] to the case of cyclic loading and fatigue of materials.

5. CALCULATION EXAMPLES

We conducted the calculations of the cyclic loading of plates with defects for the coefficient of asymmetry $R = -1$ (reverse cycle) with the formation of damage zones, appearance and development of crack-like zones of complete destruction of material particles (quasi-cracks) until their emergence at the lateral side of the plate (macrofailure).

The normal load is applied at the face ends and the lateral sides of the plate are stress-free. We consider the plane stress state. The elastic, strength, and fatigue properties of the plate material (titanium alloy) were taken from [21]: $\sigma_{\text{UTS}} = 1160$ MPa, $\sigma_{\text{f}} = 337$ MPa, $\tilde{\sigma}_{\text{f}} = 250$ MPa, $\beta_{LH} = 0.31$, and $\beta_{VH} = 0.27$. The elasticity moduli of the undamaged alloy are $\lambda_0 = 77$ GPa and $\mu_0 = 44$ GPa.

The exponent of the kinetic equation γ must be determined during matching of results of computation and fatigue experiments. For the numerical calculations in the damage equation, we took the average value $\gamma = 0.5$, $\alpha = 1 - \gamma$.

The plate dimensions are 40×40 mm. The horizontal central axis $y = 0$ and the vertical central axis $x = 0$ of the plate are the axes of symmetry; therefore, the computation was performed for the domain $x > 0$, $y > 0$. We considered the three types of defects in the middle of the plate: the circular hole with the radius $r = 1$ mm, the narrow elliptic hole with the horizontal axis $a = 1$ mm and the vertical axis $b = 0.2a$, and the narrow elliptic hole with the vertical axis $b = 1$ mm and the horizontal axis $a = 0.2b$. In Fig. 2, we show the computation results for the circular hole. In this and subsequent figure, we present the contour lines of the maximal principal stress around the quasi-crack at the instance when it passes approximately a half of the distance to the lateral side. In the figure captions, we mention the number of cycles: N_i until the initiation of failure, N_f until the macrofailure, and N_k for the position presented in the graph. We also mention the maximal level of tensile stresses P in the cycle of applied loads and the corresponding mode of fatigue damage.

In Fig. 3, we show the computation results for the horizontally oriented narrow elliptic hole. In Fig. 4, we show the results for the vertically oriented narrow elliptic hole.

Note that the number of cycles N_k corresponding to the level of advance of the crack-like zones of material particle damage (quasi-cracks) approximately until the middle of the sample (Figs. 2–4) is rather close to the number of cycles N_f, which indicates the subsequent final high-speed process of macrofailure.

From the figure, we see that the close level of cyclic loads applied to samples with defects of different types and orientation may lead to the sample fatigue macrofailure in completely different modes. For instance, for the vertically oriented elliptic defect, at the level $P = 264$ MPa, we have the mode transition to VHCF (Fig. 4a) with the lifetime $N_f = 4.709 \times 10^7$. While for the horizontally oriented elliptic defect,

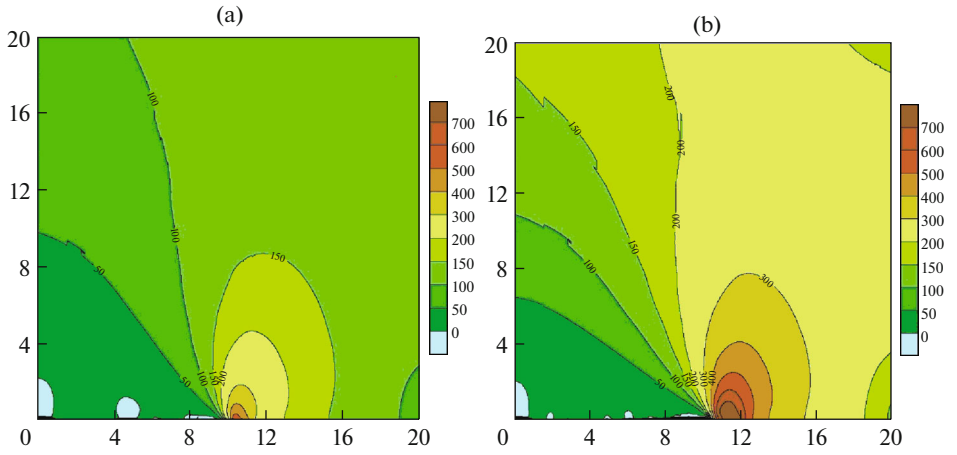

Fig. 3. (a) VHCF mode: $P = 100$ MPa, $N_k = 1.350 \times 10^9$, $N_i = 2.903 \times 10^4$, and $N_f = 1.351 \times 10^9$ and (b) HCF mode: $P = 180$ MPa, $N_k = 1.009 \times 10^6$, $N_i = 1.971 \times 10^4$, and $N_f = 1.057 \times 10^6$.

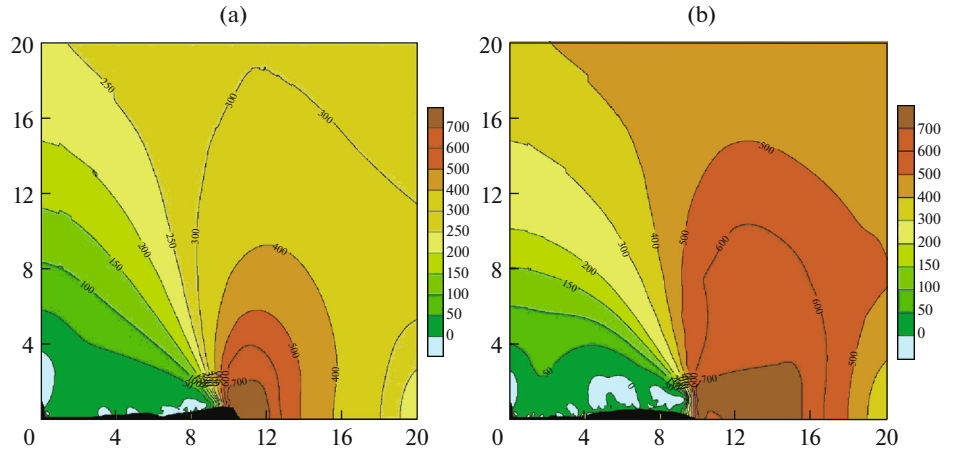

Fig. 4. (a) VHCF mode: $P = 264$ MPa, $N_k = 4.893 \times 10^7$, $N_i = 2.619 \times 10^7$, and $N_f = 4.896 \times 10^7$ and (b) HCF mode: $P = 400$ MPa, $N_k = 9.659 \times 10^5$, $N_i = 8.701 \times 10^5$, and $N_f = 9.776 \times 10^5$.

at considerably lower $P = 180$ MPa, macrofailure occurs by the HCF mechanism (Fig. 3b) with the lifetime $N_f = 1.057 \times 10^6$.

Also, in the computation with multimode model, we revealed and modeled the effect observed in fractographic studies of structural elements destructed at operation [33]. For a relatively low level of applied loads, the initiation and the initial development of the fatigue damage zones follow the VHCF mechanism because of internal defects. Furthermore, at the concentration and growth of stress levels near the front of the propagating quasi-crack, a transition to another branch (LCF–HCF) of the fatigue curve occurs. Here, the rate of the fatigue damage development changes dramatically.

The developed multimode model and numerical method allow performing the direct computation for the development of fatigue damage and crack-like zones without explicit separation of cracks in their classical sense, as well as estimating the lifetime of samples from the appearance of first nuclei to the macrofailure.

CONCLUSIONS

We proposed the multimode kinetic model of damage development at cyclic loading for describing the process of fatigue fracture. To determine the coefficients of the kinetic damage equation, we used the well-

known SWT criterion of multiaxial fatigue fracture, where the mechanism related with development of microcracks is embedded. On this basis, we proposed the procedure for computing the coefficients of the kinetic equation for different modes of fatigue destruction: LCF–HCF and VHCF.

We developed the unified numerical method and provided computation examples of development of crack-like damage zones and fatigue fracture of samples containing various defects for different modes of cyclic loading from LCF to VHCF.

FUNDING

The work was supported by the Russian Science Foundation, project no. 19-19-00705.

REFERENCES

1. O. H. Basquin, "The exponential law of endurance tests," Proc. Amer. Soc. Test. Mater. **10**, 625–630 (1910).
2. G. Sines, Behavior of Metals under Complex Static and Alternating Stresses. Metal Fatigue (McGraw-Hill, New York, 1959), pp. 145–169.
3. B. Crossland, "Effect of large hydrostatic pressures on torsional fatigue strength of an alloy steel," in *Proc. Int. Conf. on Fatigue of Metals* (London, 1956), pp. 138–149.
4. W. Findley, "A theory for the effect of mean stress on fatigue of metals under combined torsion and axial load or bending," J. Eng. Ind. **81** (4), 301–306 (1959).
5. F. Morel, "A critical plane approach for life prediction of high cycle fatigue under multiaxial variable amplitude loading," Int. J. Fatigue **22** (2), 101–119 (2000).
6. T. Matake, "An explanation on fatigue limit under combined stress," Bull. JSME **20**, 257–263 (1977).
7. D. L. McDiarmid, "A shear stress based critical-plane criterion of multiaxial fatigue failure for design and life prediction," Fatigue Fract. Eng. Mater. Struct. **17**, 1475–1484 (1999).
8. I. V. Papadopoulos, "Long life fatigue under multiaxial loading," Int. J. Fatigue **23**, 839–849 (2001).
9. A. Carpinteri, A. Spagnoli, and S. Vantadori, "Multiaxial assessment using a simplified critical plane based criterion," Int. J. Fatigue **33**, 969–976 (2011).
10. M. A. Meggiolaro, A. C. Miranda, and J. de Castro, "Comparison among fatigue life prediction methods and stress-strain models under multiaxial loading," in *Proc. 19th Int. Congress on* Mechanical Engineering (Brazilia, 2007).
11. Ying-Yu Wang and Wei-Xing Yao, "Evaluation and comparison of several multiaxial fatigue criteria," Int. J. Fatigue **26**, 17–25 (2004).
12. A. Karolczuk, J. Papuga, and T. Palin-Luc, "Progress in fatigue life calculation by implementing life-dependent material parameters in multiaxial fatigue criteria," Int. J. Fatigue **134**, 105509 (2020).
13. N. G. Bourago, A. B. Zhuravlev, and I. S. Nikitin, "Models of multiaxial fatigue fracture and service life estimation of structural elements," Mech. Solids **46** (6), 828–838 (2011).
14. P. C. Paris and F. Erdogan, "Critical analysis of crack propagation laws," J. Basic Eng. **85**, 528–533 (1963). https://doi.org/10.1115/1.3656900
15. J. A. Collins, *Failure of Materials in Mechanical Design: Analysis, Prediction, Prevention* (Wiley, New York, 1993).
16. V. N. Shlyannikov, "Creep-fatigue crack growth rate prediction based on fracture damage zones models," Eng. Fract. Mech. **214**, 449–463 (2019).
17. L. M. Kachanov, "O vremeni razrusheniya v usloviyakh polzuchesti," Izv. Akad. Nauk SSSR Otd. Tekh. Nauk **8**, 26–31 (1958).
18. Yu. N. Rabotnov, "O mekhanizme dlitel'nogo razrusheniya," in @Voprosy prochnosti materialov i konstruktsii@ (USSR Acad. Sci., Moscow, 1959), pp. 5–7.
19. S. Murakami, *Continuum Damage Mechanics. A Continuum Mechanics Approach to the Analysis of Damage and Fracture* (Springer, Dordrecht, 2012).
20. J. Lemaitre and J. L. Chaboche, *Mechanics of Solid Materials* (Univ. Press, Cambridge, 1994).
21. A. K. Marmi, A. M. Habraken, and L. Duchene, "Multiaxial fatigue damage modeling at macro scale of Ti_6Al_4V alloy," Int. J. Fatigue **31**, 2031–2040 (2009).
22. Zhi Yong Huang, D. Wagner, C. Bathias, and J. L. Chaboche, "Cumulative fatigue damage in low cycle fatigue and gigacycle fatigue for low carbon-manganese steel," Int. J. Fatigue **33**, 115–121 (2011).
23. O. Plekhov and O. Naimark, et al., "The study of a defect evolution in iron under fatigue loading in gigacycle fatigue regime," Fratt. Integrita Strutturale **10** (35), 414–423 (2016).
24. N. G. Burago and I. S. Nikitin, Multiaxial fatigue criteria and durability of titanium compressor disks in low- and giga- cycle fatigue modes," in *Mathematical Modeling and Optimization of Complex Structures* (Springer, Heidelberg, 2016), pp. 117–130.

25. A. A. Shanyavskiy and A. P. Soldatenkov, "The fatigue limit of metals as a characteristic of the multimodal fatigue life distribution for structural materials," Proc. Struct. Integr. **23**, 63–68 (2011).
26. R. N. Smith, P. Watson, and T. H. Topper, "A stress-strain parameter for the fatigue of metals," J. Mater. **5** (4), 767–778 (1970).
27. N. Gates and A. Fatemi, "Multiaxial variable amplitude fatigue life analysis including notch effects," Int. J. Fatigue **91**, 337–351 (2016).
28. N. G. Burago and I. S. Nikitin, "Matrix-free conjugate gradient implementation of implicit schemes," Comput. Math. Math. Phys. **58** (8), 1247–1259 (2018).
29. N. G. Burago, I. S. Nikitin, A. D. Nikitin, and B. A. Stratula, "Algorithms for calculation damage processes," Fratt. Integrita Strutturale **49**, 212–224 (2019).
30. N. G. Burago and I. S. Nikitin, "Algoritmy skvoznogo scheta dlya protsessov razrusheniya," Komp'yut. Issled. Model. **10** (5), 645–666 (2018).
31. N. G. Burago, I. S. Nikitin, and A. D. Nikitin, "Algorithms for calculating contact problems in the solid dynamics," in *Advances in Theory and Practice Computational Mechanics,* Ed. by L. C. Jain (Springer, Singapore, 2020), pp. 185–198.
32. N. G. Burago and I. S. Nikitin, "Mathematical model and algorithm for calculating pressing and sintering," Mat. Models Comput. Simul. **11** (5), 731–740 (2019).
33. A. A. Shanyavskii, *Modelirovanie ustalostnykh razrushenii metallov* (Monografiya, Ufa, 2007) [in Russian].

Translated by E. Oborin